(2) Aminabhavi, T. M.; Manjeshwar, L. S.; Balundgi, R. H.; Muddapur, M. V. *Indian J. Chem.* **1987**, *26A*, 106.
(3) Aminabhavi, T. M.; Manjeshwar, L. S.; Balundgi, R. H. *J. Chem. Eng. Data* **1987**, *32*, 50.
(4) Riddick, A. J.; Bunger, B. W. *Techniques of Organic Chemistry*, 23rd ed.; Wiley-Interscience: New York, 1970; Vol. IIA.
(5) Vogel, A. I. *A Textbook of Practical Organic Chemistry*; English Book Society-Longmans: London, 1983.
(6) Gokavi, G. A.; Raju, J. R.; Aminabhavi, T. M.; Balundgi, R. H.; Muddapur, M. V. *J. Chem. Eng. Data* **1986**, *31*, 15.
(7) Kell, G. S. *J. Chem. Eng. Data* **1975**, *20*, 97.
(8) Grunberg, L. *Trans. Faraday Soc.* **1954**, *50*, 1293.
(9) "American Petroleum Institute Research Project 44"; Chemical Thermodynamic Properties Center, Texas A&M University, College Station, TX (see Table 5a dated Oct. 31, 1950).
(10) Fort, R. J.; Moore, W. R. *Trans. Faraday Soc.* **1965**, *61*, 2102.
(11) Fort, R. J.; Moore, W. R. *Trans. Faraday Soc.* **1966**, *62*, 1112.
(12) Timmermans, J. *Physico-Chemical Constants of Pure Organic Compounds*; Interscience: New York, 1950.
(13) *CRC Handbook of Chemistry and Physics*, 64th ed.; Weast, R. C., Ed.; CRC: Boca Raton, FL, 1983-84.
(14) Snyder, L. R.; Kirkland, J. J. *Introduction to Modern Liquid Chromatography*; Wiley: New York, 1976; Chapter 6.

Received for review August 11, 1986. Revised manuscript received April 4, 1987. Accepted May 19, 1987.

Modelling of Impurity Effects in Fluids and Fluid Mixtures

John S. Gallagher* and Graham Morrison

National Bureau of Standards, Gaithersburg, Maryland 20899

An extended corresponding-states model of the Helmholtz free energy for two-component mixtures, based upon existing accurate representations of the principal component as the reference function, has been used to model the effects of impurities. The results give a clearer and more accurate view of the errors in the measurement of thermodynamic properties caused by small amounts of impurity. The model is also extended to include three-component mixtures to allow the estimation of the effects of impurities in two-component mixtures. The model is applied to two systems of practical importance: methane as an impurity in ethylene, and *n*-butane as an impurity in isobutane–isopentane mixtures. Both of these systems are of commercial importance and commonly used in their critical regions, where the effect of impurities on thermodynamic values is large, and where existing procedures for the estimation of the impurity effects are not accurate. New experimental determinations of the critical line for ethylene containing small amounts of methane have improved the ability to predict the behavior of the impure ethylene near its critical point.

Introduction

There is a growing awareness of the need for more accurate methods for the prediction of properties of fluids used in commercial quantities where there are likely to be significant amounts of impurities, particularly if the region of use of the material is near the critical region. In custody transfer, for instance, the density ρ of the fluid is often calculated, at measured pressure p and temperature T, from a known equation of state formulation. In the limit of infinite dilution, $x \rightarrow 0$, where x is the mole fraction of impurity

$$(\partial V/\partial x)_{pT} = VK_T(\partial p/\partial x)_{VT} \quad (1)$$

where K_T is the compressibility of the pure fluid. $(\partial p/\partial x)_{VT}$, in general, is a finite quantity. At the critical point of the pure fluid, it reaches the value

$$(\partial p/\partial x)_{VT} = \mathrm{d}p/\mathrm{d}x|_{\mathrm{crl}} - \mathrm{d}p/\mathrm{d}T|_{\sigma}^{\mathrm{c}}\, \mathrm{d}T/\mathrm{d}x|_{\mathrm{crl}} \quad (2)$$

where $\mathrm{d}p/\mathrm{d}x|_{\mathrm{crl}}$ and $\mathrm{d}T/\mathrm{d}x|_{\mathrm{crl}}$ are the initial slopes of the critical line of the mixture in $p-x$ and $T-x$ space, respectively, and $\mathrm{d}p/\mathrm{d}T|_{\sigma}^{\mathrm{c}}$ is the limiting slope of the solvent's vapor pressure curve. Thus, the change in molar volume, at constant p and T, due to a small admixture x is

$$\delta V = (\partial V/\partial x)_{pT}x + \ldots \quad (3)$$
$$\propto xK_T$$

Equation 3 is based on a Taylor expansion at constant p,T (*1-4*). It shows that the effect of the impurity on molar volume or molar density is proportional to the solvent's compressibility, and therefore becomes very large in the critical region. The compressibility diverges at the critical point, where expression 3 becomes invalid. It therefore seems worthwhile to model the impurity effects by means of a Helmholtz free energy representation for the mixture. As long as this is done in a consistent way, a classical equation of state for the major component, combined with the classical principle of corresponding states, the impurity effects can be calculated at any point in the $p-T$ plane. We find that impurity effects on the density are very large and not linear in x in a large region around the critical point of the fluid. Also, we find that impurities can induce a phase transition and therefore, if the pure-fluid equation of state is used, one may even predict the wrong phase.

The two examples studied here are that of ethylene, for the purpose of custody transfer, and that of a 90%-10% isobutane–isopentane mixture used in a Rankine cycle for geothermal power generation. Ethylene is produced in very large quantities and is transferred from producer to consumer through pipelines in which the fluid, whose critical temperature is 9 °C, may assume conditions not too far from criticality. Commercial ethylene is at least 99.85% pure, the most volatile contaminant being methane. We will estimate the errors in the density, at given pressure and temperature, caused by a worst-case scenario of 0.15 mol % methane. Another system modelled is the isobutane–isopentane mixture containing *n*-butane as an impurity. These mixtures are used as working fluids in geothermal binary power cycles, and the interest here is in the effect of impurities on the thermodynamic properties of the working fluid which affect the efficiency of the power cycle. Since the commercial grade of isobutane, the major component of the mixture, may contain up to 5% impurity, principally *n*-butane, the location of the critical point and the phase boundaries can be significantly affected. Before extending the treatment to the 3-component system, we calculate the effect of a small amount of isopentane in pure isobutane.

In both of the examples we have the advantage of the availability of an excellent classical equation of state for the major component. Using this equation as a reference, we have modelled the mixture properties using principles of extended corresponding states.

Table I. The Critical Parameters of the Fluids Discussed in this Report

fluid	T^c, K	P^c, MPa	ρ^c, mol/dm^3	MW, g/mol
ethylene	282.345	5.0401	7.634	28.054
methane	190.555	4.5988	10.321[a]	16.043
isobutane	407.84	3.629	3.880	58.124
isopentane	460.51	3.371	3.192[a]	72.151
n-butane	425.16	3.796	3.893[a]	58.124

[a] These densities are calculated by equating the critical compressibility factors to that of the reference fluid.

The Mixture Model

The first step in the construction of a Helmholtz function $A(\rho,T,x)$ for a mixture, where a reference Helmholtz function for one of the components has already been chosen, is the generation of a Helmholtz function for the second component by means of the principles of corresponding states. A discussion of these principles by Rowlinson et al. can be found in ref *5*. Our goal is to map the coexistence curve of the second component onto the coexistence curve of the reference function by using the critical point as the key value for the correspondence. For convenience and simplification of the equations, all quantities used will be expressed in reduced form, where the reduction factors are the critical point values for the reference material. Table I shows the measured values of the critical parameters for the substances discussed in this paper. In all equations to follow, the bar over the name of a variable will be used to denote these reduced quantities. The use of the asterisk as a superscript to a quantity will indicate a reduction parameter. (A single asterisk indicates a primary reduction factor, and a double asterisk a derived reduction factor.) Thus, the primary reduction factors are T^*, p^*, and ρ^*, for which we will use the T^c, p^c, and ρ^c of the reference fluid; and the derived reduction factors will include A^{**} $(=p^*/\rho^*)$, S^{**} $(=A^{**}/T^*)$, and the reduced gas constant $R^{**} = R/S^{**}$. For example, $\bar{T} = T/T^*$, $\bar{p} = p/p^*$, $\bar{\rho} = \rho/\rho^*$, $\bar{A} = A/A^{**}$, and $\bar{G} = G/A^{**}$.

If we define the following ratios (where the subscript 1 refers to the reference fluid and 2 to the second component of the mixture)

$$f_0 = \bar{T}_2^c/\bar{T}_1^c$$

$$h_0 = \bar{V}_2^c/\bar{V}_1^c = \bar{\rho}_1^c/\bar{\rho}_2^c$$

$$q_0 = \bar{p}_2^c/\bar{p}_1^c \qquad (4)$$

the principle of corresponding states postulates that, for all values of V and T

$$Z_2(\bar{V}_2,\bar{T}_2) = Z_1(\bar{V}_1=\bar{V}_2/h_0,\ \bar{T}_1=\bar{T}_2/f_0)$$

$$\bar{A}_2^f(\bar{V}_2,\bar{T}_2) = f_0\bar{A}_1^f(\bar{V}_1=\bar{V}_2/h_0,\ \bar{T}_1=\bar{T}_2/f_0) - R^{**}\bar{T}_2 \log(h_0) \qquad (5)$$

where Z is the compressibility factor pV/RT $(=\bar{p}\bar{V}/R^{**}\bar{T})$ and $\bar{A}^f$ is the configurational portion of the Helmholtz function $\bar{A}^f = \bar{A} - \bar{A}_0$. ($\bar{A}_0$ is the ideal gas contribution to the Helmholtz function.) These relations imply that $f_0 = h_0q_0$. Since, in general, two substances do not have exactly the same critical compressibility, and the critical density is the least well determined of the three critical parameters, we will define the h_0 as f_0/q_0, thus in effect defining a new critical density of the second fluid such that the critical compressibility factor will be the same as that of the reference fluid.

Our model also includes the ability to make use of functions designed to improve the prediction of the vapor pressures and coexisting densities of the second fluid, such as the "shape factors" of Leach et al. (*7*) and Rowlinson and Watson (*6*). These are used for the Helmholtz function for the isobutane–isopentane mixture described later, but for the purposes of estimating impurity effects, where the concentration of the "impurity" component is very small, their contribution to the values calculated from the model can safely be ignored.

The extension of this procedure to the generation of a Helmholtz function for a mixture again follows principles described by Rowlinson and Watson (*6*), and is referred to as the "one-fluid" model. If we let x be the mole fraction of the second component, we can define the corresponding-states principle through a pair of equations equivalent to (5) but with the subscripts "2" replaced by "x" (where the subscript x refers to a property of a mixture with a mole fraction x of the second component). The T_x^c, p_x^c, and V_x^c will be defined as functions of x and of the T^c, p^c, and V^c for each of the two pure fluids through "mixing rules" of the van der Waals type

$$\bar{V}_x^c = (1-x)^2\bar{V}_1^c + 2x(1-x)\bar{V}_{12}^c + x^2\bar{V}_2^c$$

$$\bar{T}_x^c = (1-x)^2\bar{T}_1^c + 2x(1-x)\bar{T}_{12}^c + x^2\bar{T}_2^c \qquad (6)$$

where the $\bar{V}_{12}^c$ and $\bar{T}_{12}C$ are defined by the "combining rules"

$$\bar{V}_{12}^c = k[\tfrac{1}{2}(\bar{V}_1^c)^{1/3} + \tfrac{1}{2}(\bar{V}_2^c)^{1/3}]^3$$

$$\bar{T}_{12}^c = \ell[\bar{T}_1^c\,\bar{T}_2^c]^{1/2} \qquad (7)$$

(k and ℓ are adjustable parameters for the modification of the location of the pseudocritical line. In our model they will be simple constants, with numerical values near unity.)

These combining rules are among the simpler of the many such rules that have been proposed, and have been found to be as adequate for simple fluids as the more complex ones. These mixing rules and combining rules together define a critical line between the critical points of the two pure fluids. This line is not the real critical line, but is related to it, and is referred to as the pseudocritical line (see the next section).

The definitions of the f_x, h_x, and q_x follow from the definitions of the f, h, and q already seen in eq 4 and 5 with the substitution of $\bar{T}_x^c$, $\bar{p}_x^c$, and $\bar{\rho}_x^c$ for the $\bar{T}_2^c$, and $\bar{p}_2^c$, and $\bar{\rho}_2^c$. With these functions now defined, the corresponding-states relations for the mixture can be written as

$$Z_x(\bar{V}_x,\bar{T}_x) = Z_1(\bar{V}_1=\bar{V}_x/h_x,\ \bar{T}_1=\bar{T}_x/f_x)$$

$$\bar{A}_x^f(\bar{V}_x,\bar{T}_x) = f_x\bar{A}_1^f(\bar{V}_1=\bar{V}_x/h_x,\ \bar{T}_1=\bar{T}_x/f_x) - R^{**}\bar{T}_x \log(h_x) \qquad (8)$$

All thermodynamic properties may be calculated from this Helmholtz function, in the same manner as done for pure fluids, by taking derivatives with respect to $\bar{T}$ and $\bar{V}$. (We will also need to calculate chemical potentials, which will require derivatives with respect to x, which we can calculate numerically.)

Determination of the Critical Line and the Dew and Bubble Points

The critical point for a pure fluid is defined as that point where $(\partial p/\partial\rho)_T$ and $(\partial^2 p/\partial\rho^2)_T$ are simultaneously zero because of incipient mechanical instability. In a mixture, the use of this criterion would define a line of points T_x^c, V_x^c, and P_x^c through eq 8. The line just described is often referred to as the pseudocritical line: that is, the line of critical points where the composition is constrained to be the same on each side of the coexistence boundary. However, in a mixture, the liquid and vapor phases would separate at a somewhat higher temperature because of incipient material instability. The "real" critical line is defined as the line of points where $(\partial\mu/\partial x)_{p,T}$ and $(\partial^2\mu/\partial x^2)_{p,T}$ are simultaneously zero. This set of conditions is equivalent to the requirement that $(\partial^2 G/\partial x^2)_{p,T}$ and $(\partial^3 G/\partial x^3)_{p,T}$ be simultaneously zero. This point can be calculated through the use of numerical derivatives in the following manner: first, the temperature is chosen, and at this temperature a trial value of x is chosen. At this T and x, a table is calcu-

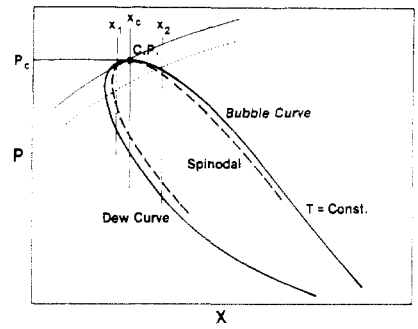

Figure 1. Diagram showing a liquid–vapor phase boundary for a constant temperature. The dashed line represents the locus of points for which $(\partial^2 G/\partial x^2)_{Tp} = 0$, which coincides with the liquid–vapor phase boundary at the critical point for that temperature, and the dotted line represents the "pseudocritical" line.

lated of p and $(\partial^2 G/\partial x^2)$ for a range of densities and the density found from this table where, for the chosen T and x, the second derivative is zero. Repeating this procedure for the same T, (but for other values of x), one generates a line (called by van der Waals a "spinodal"). It can be shown that this line must lie within the two-phase region but be tangent to it at the point of maximum pressure, which is the critical point for this value of T. In Figure 1, we show a diagram of such a calculation. The figure shows p as a function of x for the real critical line, shown as a solid line, the pseudocritical line as dots, the "spinodal" as determined above as dashes, and the line of bubble and dew points as a solid line. (The calculation of the bubble and dew points will be discussed next.) It can be seen from this figure that the spinodal line and the bubble- and dew-point lines are tangent at the point of maximum pressure, and that this defines a point on the real critical line.

In order to calculate coexisting dew and bubble points we make use of the principle that for the liquid and vapor to be in equilibrium, the chemical potential of each component must be the same on each side of the phase boundary. That is, for each component i

$$\mu_{iL}(p,T,x_{iL}) = \mu_{iV}(p,T,x_{iV}) \qquad (9)$$

Since the chemical potentials can be calculated from the Helmholtz function, eq 9 becomes a set of nonlinear equations, one for each component of the mixture. The solutions to the set of equations at a specified T and p were obtained by using a standard package for the solution of a system of nonlinear equations. For a two-component mixture, since the concentration of the second component in each phase is unity less the concentration of the first component, the fixing of T and p completely determines the solution. (For three components, the solution requires the specification of one more quantity such as the concentration of one of the components on one side of the phase boundary.)

Methane in Ethylene

Ethylene is a material of considerable commercial importance. Unfortunately for the community of producers and consumers of this substance, the critical temperature (282.3 K) is in the range of ambient temperatures at which this material is usually handled, and it is within the critical region where the traditional methods of approximating the impurity effects come into difficulties. Since a Helmholtz function accurately representing the properties of pure ethylene has recently been published (*8*), we can model the effects of small amounts of methane (the principal volatile impurity in commercial lots) in ethylene through the use of the methods just discussed. Since the amount of methane will never be as large as 1%, it will not be necessary to determine shape factors to represent the vapor pressure and coexisting densities of pure methane accurately,

Table II. Measured Points on the Ethylene–Methane Critical Line

mole fracn methane	$(P^c - P^c_{C_2H_4})$, MPa	$(T^c - T^c_{C_2H_4})$, K
0.0	0.0	0.0
0.016	0.0294	−0.099
0.034	0.0859	−2.164
0.057	0.1773	−3.427
0.073	0.246	−5.485
0.0965	0.385	−6.167
0.0822	0.334	−5.262
0.0646	0.211	−4.063
0.0680	0.219	−4.310

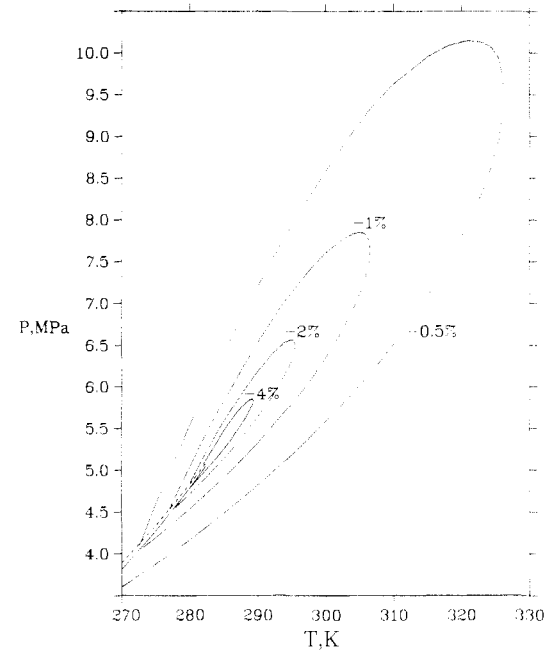

Figure 2. Contours representing the locus of points where the molar density difference between pure ethylene and ethylene containing 0.15 mol % methane is as indicated.

and we have set the shape factors to unity. Similarly, since the modelling of pVT relationships make no use of the ideal-gas functions, it is not necessary to include the pure-methane ideal-gas functions.

The locus of critical temperatures and pressures for mixtures of ethylene with small amounts of methane ($x < 0.10$) were measured because of the inadequacy of available data in this region. The mixtures were prepared on a gas buret with research grade materials (ethylene (Matheson), $x = 0.9998$; methane (Phillips), $x = 0.9998$). The analyses of the mixtures were determined both gravimetrically and by gas chromatography; the uncertainty in the methane composition was ±0.0001 in mole fraction. The samples were contained in a small variable volume sapphire cell designed for measuring critical points (*9*); the temperature was controlled to ±0.0003 K during the measurements. The uncertainty in the measured critical temperature was 0.003 K and the uncertainty of the pressures 2 kPa. As indicated by the data, shown in Table II, the addition of methane to ethylene causes the critical pressure to rise and the temperature to fall. There is no indication that the critical locus is collinear with the ethylene saturation line at the ethylene critical point or that there is a temperature maximum in the locus except at the ethylene critical point.

The rather steep rise in the critical pressure when small amounts of methane are added to ethylene requires an adjustment of the parameters of the model so that the predicted critical pressure and temperature will reflect these measurements. The adjustment of the parameters k and l in the combining functions to the values 1.106 and 0.938, respectively,

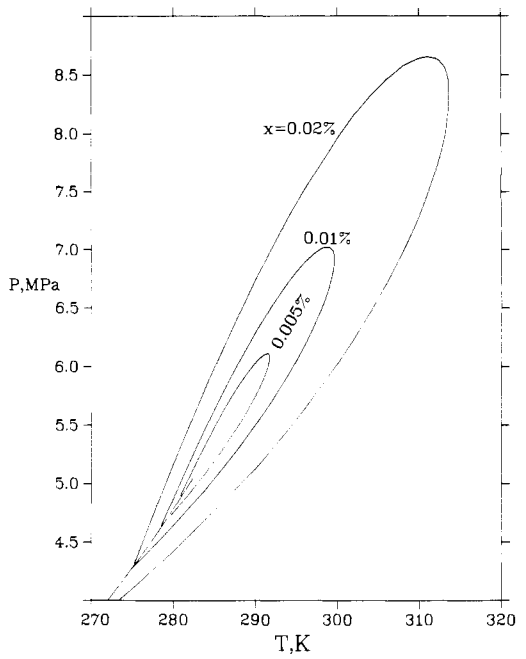

Figure 3. Contours representing the locus of points for which the addition of the specified amount of methane to pure ethylene results in difference of 0.1% in the density.

allows us to predict a critical line that closely resembles the experimental measurements, which should be more than sufficient for the purpose of predicting the pVT relationship for $x < 0.01$. The values for k and ℓ thus chosen can be seen to vary considerably from unity, but this causes no difficulty in computations. Equation 2 permits calculation of the prefactor $(\partial p/\partial x)_{VT}$ in eq 1. Our model gives a 4% smaller value than an estimate based on the observed slope of the critical line. For the purpose of an estimate of an impurity effect, this agreement is quite satisfactory.

With the choice of k and ℓ, the Helmholtz function for the mixture is completely defined. We have used this function to generate pVT relationships and calculate the dew and bubble points for small values of methane concentration corresponding to the amount of impurity that might be expected in practical operations, and compared these values with those of pure ethylene. In Figures 2 and 3, we display some of these results graphically. In both figures contours of constant differences in total molar density at given p and T between pure ethylene and ethylene with small amounts of methane added are plotted in $p-T$ space. In Figure 2 we have assumed a constant methane mole fraction of 0.0015 (0.15%) and plotted contours of errors in the total molar density of the mixture. Note the large area in $p-T$ space for which the density differences are greater than 0.5%, and a significant region for which the differences are 2% or more. Figure 3 illustrates similar information from another perspective. We see here contours representing the amount of methane required to produce a density difference of 0.1%. If this error is specified as the maximum tolerable, this figure will show which regions of $p-T$ space must be avoided for a given fraction of methane in the mixture. In both figures the vapor pressure curve for pure ethylene has also been included as a solid line ending at the critical point. Figure 2 also includes as a dashed curve the line of bubble points for the 0.15% methane in ethylene mixture, indicating the large differences that can result from such small amounts of impurity, especially at the lower temperatures. The line of dew points is close enough to the vapor pressure curve to be indistinguishable at the scale of this figure. Figure 4 shows, in a somewhat more conventional manner on a volume vs. methane concentration plot, lines of constant temperature and pressure. The temperature chosen for this plot, 282 K, is a fraction of a degree below the critical temperature for pure ethylene, and the pressures cover a range from below to above the critical pressure. Note the large changes of volume that can occur with the addition of quite small amounts of methane.

An Impurity in a Two-Component Mixture: *n*-Butane in Isobutane–Isopentane

As an example of the extension of these principles to calculate impurity effects in a mixture, we will consider the system of isobutane–isopentane mixtures with small amounts of *n*-butane present as an impurity. This system is of practical importance, as the isobutane–isopentane mixtures have been proposed as the working fluid for power generation from geothermal sources in a binary power cycle. The choice of the ratio of these two substances allows the power plant designer to alter the properties of the mixture to match the available external conditions for maximum efficiency. Since the materials will be used in large quantities, it is not economically feasible to specify high purities. The specifications of the commercial

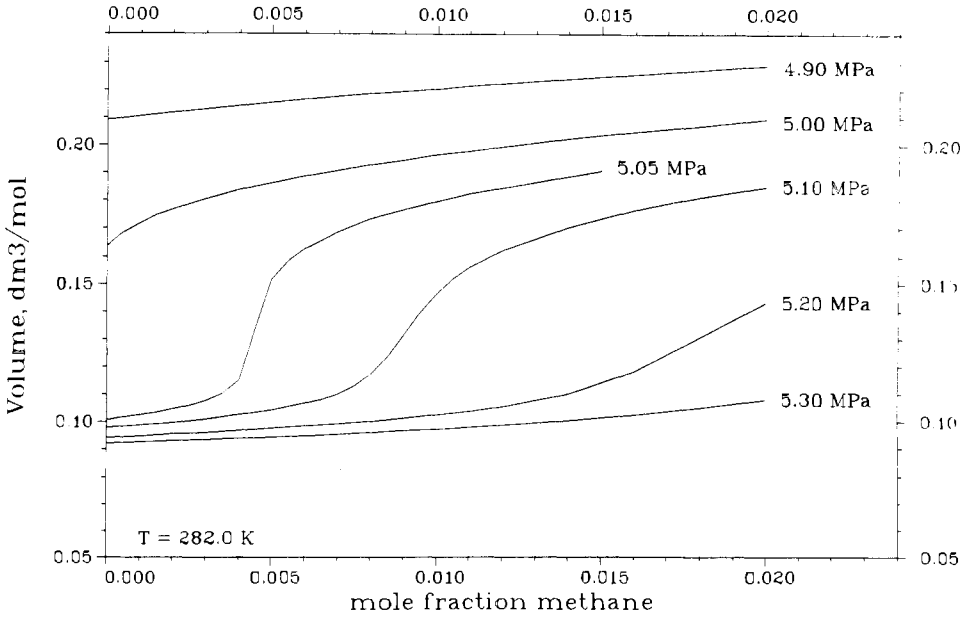

Figure 4. Calculated volume along isotherm–isobars of ethylene containing the specified mole fraction of methane.

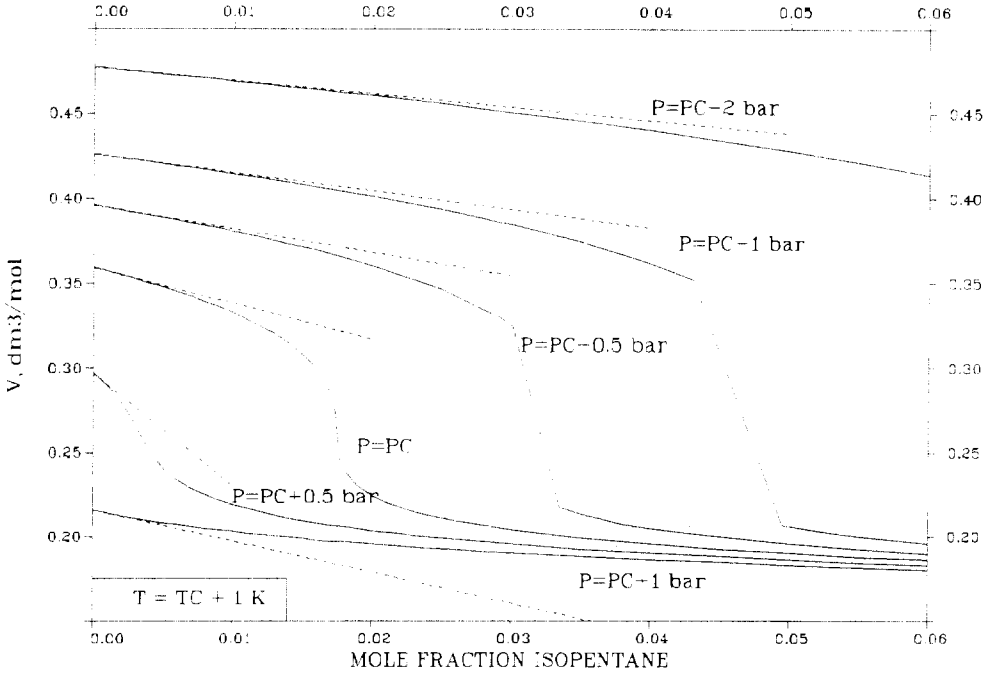

Figure 5. Calculated volume along an isotherm–isobar for pure isobutane containing the specified mole fraction of isopentane. The dashed lines indicate the predicted volumes using the Taylor expansion method: this method gives the correct initial slope but not the deviations from this slope as the concentration of impurity increases.

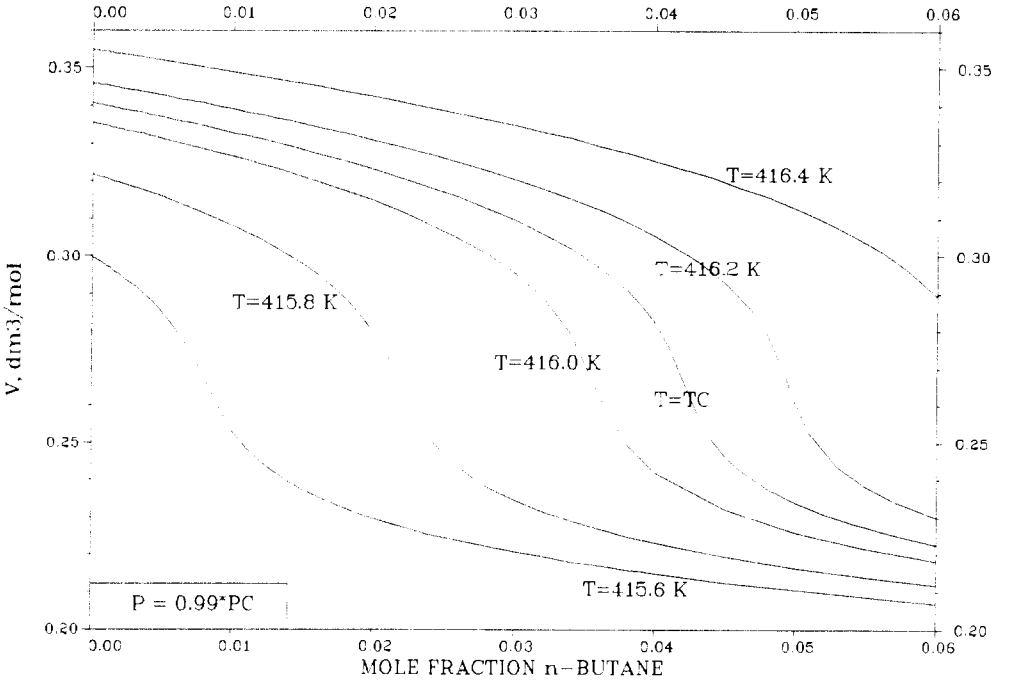

Figure 6. Calculated volumes along isotherm–isobars for *n*-butane added to a 90% isobutane–10% isopentane mixture as an impurity.

grades of isobutane and isopentane allow for as much as 5% impurity, principally other isomers of the material being purchased, and the predicted properties of the mixture can be significantly affected. Since the principal component of the mixture used is isobutane (typically 90%), the resulting working fluid may contain up to 4–5% of *n*-butane, and this is the three-component mixture we will consider.

The two-component isobutane–isopentane mixture model using these methods has been described in detail (*10*) based upon an equation of state for isobutane as the reference fluid (*11*). Using the extension of the model to a three-component mixture as described in an earlier section, we can make the following simplifying assumptions: First, since the concentration of *n*-butane can be assumed never to be more than 5% as in the case of methane in ethylene, we do not need to find shape factors to reproduce the pure *n*-butane vapor pressure and dew–bubble curves closely. Second, since the critical line for isobutane–*n*-butane mixtures is not expected to be unusual in any way, we can use the simplest form for the parameters k and ℓ in the combining functions (that is, $k = \ell = 1$). Solutions of the three simultaneous equations for the equality of the chemical potentials of each component on each side of the phase boundary can now be found with the specification of the composition of one side of the phase boundary.

Some of the results of calculations made from this model are displayed in figures 5 through 9. In Figure 5 we first show the effects of the addition of small amounts of isopentane to isobutane using the two-component model. The quantity plotted is the specific volume of the mixture as a function of the concentration of the added isopentane. The solid curves are for

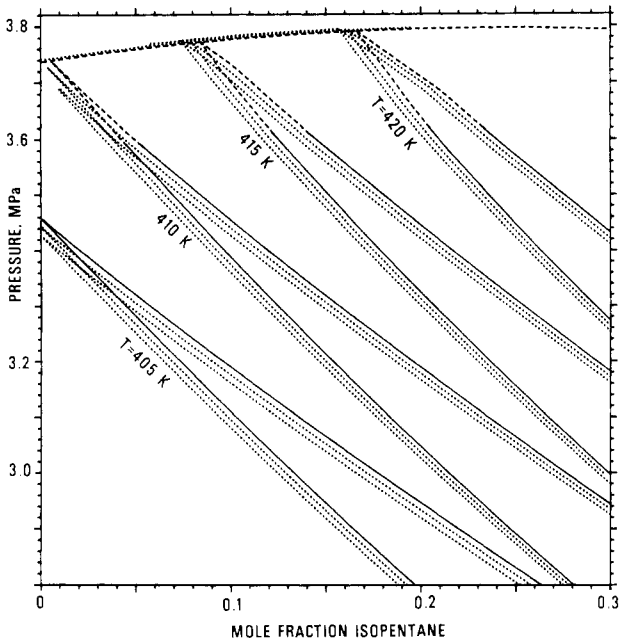

Figure 7. Dew–bubble curves for isobutane–isopentane mixtures with isopentane concentration of x, plotted as pressure vs. x. The dotted lines represent the same isotherms but where the isobutane in the mixture contains 2% and 4% n-butane.

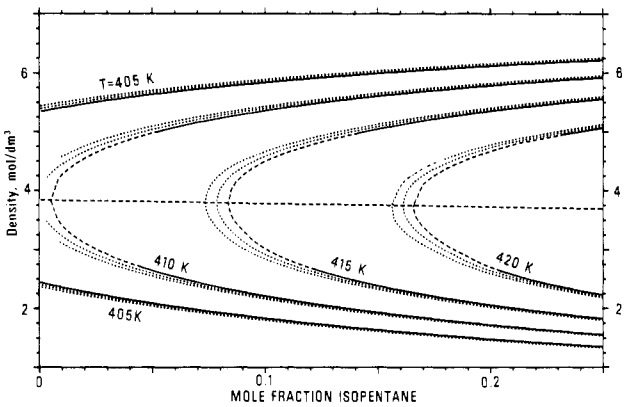

Figure 8. Dew–bubble curves as in Figure 6 but plotted as molar density vs. x. Note that for T near the critical temperature of the isobutane–isopentane mixture, the densities change most severely with the addition of the n-butane.

constant T and p, and the dashed lines represent similar calculations made by the Taylor expansion (*1*). This method gives acceptable results except in and just above the critical region. Note that the calculated molar volumes for just 1 or 2% of isopentane can be in error by 10 or 20%, or even result in the prediction of the wrong phase, and that the molar volumes do not vary linearly with the addition of impurities, as would be predicted by the truncated Taylor expansion. In Figure 6 we show a similar plot, but where the impurity is n-butane added to a 90% isobutane-10% isopentane mixture, where the isobutane/isopentane ratio is held constant as well as p and T, representing conditions that might be found in power cycles in geothermal power generation. The effects of this impurity are similar to those shown for the small amounts of isopentane in isobutane, except that the phase transitions are not as sharp.

The line of dew points and bubble points has also been determined for this mixture. We show in Figure 7 these lines plotted for isotherms in the pressure–concentration plane, and in Figure 8 as density vs. concentration. The solid lines represent a 90% isobutane–10% isopentane mixture, and the dashed lines represent this mixture but where the isobutane contains 2% and 4% n-butane as an impurity. Figure 9 is a

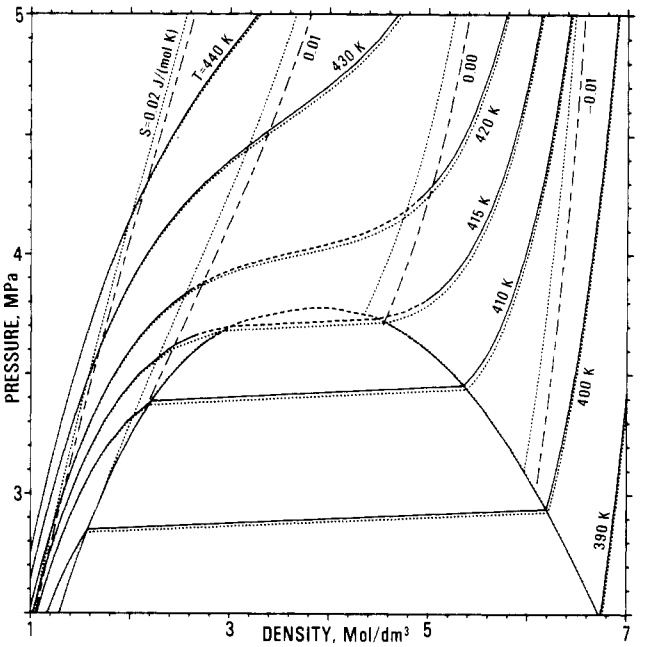

Figure 9. Isotherms, isentropes, and the dew–bubble curves for a 90% isobutane–10% isopentane mixture in the pressure vs. density plane (solid and dashed curves) and the same quantities but where the isobutane contains 2% n-butane plotted as dotted lines.

section of a pressure vs. density chart. Again the material is the 90% isobutane–10% isopentane mixture being used as the working fluid in geothermal power plants. The lines represent the dew and bubble points, isotherms, and isentropes. These same quantities are also shown as dotted lines where the isobutane contains 2% n-butane as an impurity. The horizontal separation of the isotherms represents the density difference with and without the impurity; the smaller the slope of the isotherm (the larger the compressibility) the greater the error in the density. The quantity of practical interest in the comparison of the isentropes is the difference in entropy between two states rather than the absolute numbers, which depend upon the choice of the reference state.

Since the values of k and ℓ used for the isobutane–isopentane mixture are very near unity, the predicted critical line does not exhibit any unusual features for small values of the concentration of the second or third component, although the actual values predicted for the critical parameters are not as accurate as would have been the case for a nonclassical model.

Conclusion

The effects of impurities on the density of a fluid or fluid mixture, at given pressure and temperature, have been shown to be disproportionately large and nonlinear in the impurity concentration in a large region around the critical point or line. Impurities can even induce phase transitions, so that their neglect may lead to prediction of the wrong phase. The use of a Taylor expansion in impurity concentration breaks down near a critical point and near a phase transition. The use of a corresponding-states Helmholtz free energy formulation for the impure fluid enables the calculation of impurity effects in a consistent manner. The only input information required beyond the Helmholtz function of the pure fluid is the initial slope of the critical line in p–x and T–x space.

Acknowledgment

This work has profited from many helpful discussions with Dr. J. M. H. Levelt Sengers and Dr. James Ely of the National Bureau of Standards, and Dr. Jan Sengers of the University of

Maryland. Drs. Majid Jahangiri and R. T. Jacobsen provided us with the Helmholtz function for ethylene.

Registry No. Ethylene, 74-85-1; methane, 74-82-8; butane, 106-97-8; isobutane, 75-28-5; isopentane, 78-78-4.

Literature Cited

(1) Keesom, W. H. *Commun. Phys. Lab. Leiden* **1901**, *75*.
(2) Keesom, W. H. *Commun. Phys. Lab. Leiden* **1902**, *79*.
(3) Verschaffelt, J. E. *Commun. Phys. Lab. Leiden* **1902**, *81*.
(4) Hastings, J. R.; Levelt Sengers, J. M. H.; Balfour, F. W. *J. Chem. Thermodyn.* **1980**, *12*, 1009.
(5) Chang, R. F.; Morrison, G.; Levelt Sengers, J. M. H. *J. Phys. Chem.* **1984**, *88*, 3389.
(6) Rowlinson, J. S.; Watson, I. D. *Chem. Eng. Sci.* **1969**, *24*, 1565.
(7) Leach, J. W.; Chappelear, P. S.; Leland, T. W. *AIChE J.* **1968**, *14*, 568
(8) Jahangiri, Majid. Doctoral Dissertation, University of Idaho College of Engineering, Moscow, ID, 1984.
(9) Morrison, G.; Kincaid, J. M. *AIChE J.* **1984**, *30*, 257.
(10) Gallagher, J. S.; Levelt Sengers, J. M. H.; Morrison, G.; Sengers, J. V. "Thermodynamic Properties of Isobutane-Isopentane Mixtures from 240 to 600 K and Up to 20 MPa"; NBSIR 84-2971, 1984.
(11) Waxman, M., Gallagher, J. S. In *Proceedings of the 8th Symposium on Thermophysical Properties*; Sengers, J. V., Ed.; ASME: New York, 1982; Vol. I, p 88.

Received for review September 12, 1986. Accepted June 3, 1987. This work was sponsored by the Department of Energy, Division of Geothermal and Hydropower Technology, San Francisco Operations Office, Oakland, California, contract DE-AI03-82SF11653.

Diffusion Coefficient of Aqueous Benzoic Acid at 25 °C

Robert A. Noulty and Derek G. Leaist*

Department of Chemistry, University of Western Ontario, London, Ontario N6A 5B7, Canada

A conductometric technique has been used to measure precise binary diffusion coefficients for aqueous benzoic acid solutions at concentrations from 0.0003 to 0.0153 mol dm^{-3} at 25 °C. As the concentration drops, dissociation of benzoic acid molecules increases the overall rate of diffusion of the solute. The concentration dependence of the measured diffusion coefficients is in good agreement with predicted behavior and yields 0.900 (±0.006) × 10^{-9} m^2 s^{-1} for the limiting diffusion coefficient of the undissociated aqueous benzoic acid molecule. The new diffusion data can be used to model dissolution of the acid, a standard procedure for determination of mass-transfer coefficients.

Introduction

Mass transfer between solid surfaces and moving fluids finds important applications in extraction, leaching, drying, ion exchange, and adsorption processes. Rate constants for these processes are frequently determined by measuring dissolution of test pieces of solid benzoic acid (*1-6*). This material is easily cast or pressed into tubes, plates, spheres, or cylinders. Its solubility in water lies in a convenient range, and the solutions can be analyzed accurately by titration with standardized base. Interfacial resistance to dissolution of the acid appears to be negligible (*2*).

Interpretation of benzoic acid dissolution rates requires solubility, viscosity, and diffusion data. Although accurate solubilities and viscosities have been reported (*7*), the diffusion data usually employed were obtained by the porous diaphragm cell method before reliable stirring (*8*) and calibration (*9*) procedures were developed. Because the solubility of benzoic acid in water is relatively low (0.0275 mol dm^{-3} at 25 °C (*7*)), the diaphragm cell measurements were made at low ionic strengths where adsorption on the diaphragm can lead to significant errors (*10*). The concentration dependence of the diffusion coefficient and the concentrations at which the measurements were made were not specified.

More recently, an optical technique, Mach-Zehnder interferometry, was used to measure diffusion of aqueous benzoic acid (*11*). But since solute concentrations are low and the changes in refractive index are correspondingly small, optical diffusion experiments are difficult to apply to benzoic acid solutions and the data lack precision. The reported linear concentration dependence of the diffusion coefficient is neither supported by theory nor observed for other weak acids (*12-14*).

These considerations prompted us to use the Harned conductometric method (*15*) to determine precise diffusion coefficients for benzoic acid. In this technique flow of solute is followed by measuring changes in electrical conductance along a column of diffusing electrolyte. Precise conductivity measurements can be made down to very low concentrations. Consequently, Harned's technique is the method of choice for studies of diffusion of dilute electrolytes.

Experimental Section

Procedure. The cells used in this work had cylindrical diffusion channels (1.278 cm diameter, 3.050 (±0.002) cm depth) which were machined from high-density polyethylene. Pairs of circular platinum electrodes (0.1 cm diameter) were cemented with epoxy into the cell walls at levels one-sixth and five-sixths of the channel height. The cells were initially filled with pure water or dilute benzoic acid solutions and sealed with lightly greased glass plates. To begin a run a known volume of stock benzoic acid solution was injected into the lower end of the solution chamber by using a calibrated precision syringe. Electrical resistances were measured every 10 000 s for 5 days with a General Radio Model 1689 automatic ac bridge. The bridge was interfaced with a Hewlett Packard Model 3488A switch unit and a Hewlett Packard Model 216 computer for data acquisition and analysis. The diffusion cells were held in a water thermostat controlled at 25.00 (±0.01) °C.

Experimental diffusion coefficients accurate to 0.2-0.4% were computed from measured resistances by using linear least-squares analysis of the slope (*12*, *14*)

$$D = -\frac{a^2}{\pi^2}\frac{d}{dt}\left[\ln (rK_B - K_T) + \ln\left(rK_B + K_T + \frac{K_a y_\pm \Lambda}{1000\alpha k_T}\right)\right] \quad (1)$$

Here a is the height of the solution column, K_T and K_B are reciprocal resistances measured at top and bottom electrodes positions at time t, and $r = K_B/K_T$ is the ratio of electrode cell constants. Λ, $y_\pm$, and α denote respectively the molar conductance, mean molar ionic activity coefficient, and the degree of dissociation of molecular benzoic acid at the final cell concentration. Values of Λ were obtained from conductances

0021-9568/87/1732-0418$01.50/0